NANO LETTERS

2005
Vol. 5, No. 10
1937−1942

Expanding the Optical Trapping Range of Gold Nanoparticles

Poul Martin Hansen,[†] Vikram Kjøller Bhatia,[‡] Niels Harrit,[‡] and Lene Oddershede*,[†]

Niels Bohr Institute, University of Copenhagen, Blegdamsvej 17, 2100 Copenhagen, Denmark, and Nano-Science Center, University of Copenhagen, Universitetsparken 5, 2100 Copenhagen, Denmark

Received July 6, 2005; Revised Manuscript Received August 17, 2005

ABSTRACT

We demonstrate stable three-dimensional (3D) single-beam optical trapping of gold nanoparticles with diameters between 18 and 254 nm. Three-dimensional power spectral analysis reveals that, for nanoparticles with diameters less than 100 nm, the trap stiffness is proportional to the volume of the particle. For larger particles, the trap stiffness still increases with size, however, less steeply. Finally, we provide numbers for the largest forces exertable on gold nanoparticles.

Gold nanoparticles are natural probes to use in advanced nanotechniques. Gold particles have found use, for example, as "plugs" connecting enzymes to electrical nanocircuits,[1] in array-based electrical detection of DNA,[2] as local heat sources causing hybridization of DNA,[3] and in self-assembled form, they can constitute electrical nanonetworks.[4] Gold nanoparticles have also been used to probe living systems, for example to monitor the motion of eucaryotic membrane proteins.[5] The chemical properties of gold allow for custom functionalization. Therefore, gold nanoparticles are particularly useful as handles for nanotechniques to probe biological systems of interest, and by applying force to the gold beads, the response of the system to the force can be investigated.

Optical tweezers serve as a highly sensitive and noninvasive force transducer capable of measuring forces and distances in the nanometer and sub-pico-Newton regime, respectively. For the study of biological systems, it is customary to attach a handle, for example, a latex or gold bead, to the system of interest, and the nanometer-scale motion as well as the forces acting on the bead can then be monitored using force-scope optical tweezers, which are typically based on a single laser beam. Multiple-beam optical tweezers, though not aimed at such precise measurements of forces and distances, have been used to create amazing structures on the nano- and micron scale.[6−8] For nano applications using gold beads, it is crucial to know which sizes of particles can be trapped and which range of forces can be exerted on a given particle size. To probe a particular system noninvasively, it can be of interest to use as small nanoparticles as possible. Optical trapping of latex beads smaller than $d = 300$ nm is difficult,[9,10] and the forces exertable on such small latex particles are significantly smaller than those on corresponding gold particles. This is another reason to use gold rather than other materials as nanoprobes.

Three-dimensional (3D) trapping of 36.2-nm gold nanoparticles was first reported by Svoboda and Block,[9] who also showed that the trapping forces on gold nanoparticles in the Rayleigh regime (diameter $d \ll$ wavelength λ) are significantly larger than on latex beads of similar size. To minimize opticution of biological specimens, optical tweezers typically use infrared lasers with wavelengths significantly longer than the resonance wavelength for gold. In the ray optics regime ($d \gg \lambda$), on the other hand, it is only possible to optically trap gold beads in 2 dimensions.[11,12,13] Three-dimensional trapping of a $d = 40$ nm gold particle has also been applied in conjunction with a scanning near-field optical microscope (SNOM).[14] In counterpropagating laser tweezers, the scattering force stabilizes rather than destabilizes the optical trap. Therefore, counterpropagating traps are likely to be well suited for trapping metallic particles.

In this letter, we demonstrate single-beam optical trapping in three dimensions of gold spheres with diameters ranging from 18 to 254 nm, thus substantially extending the previously known regime of optical trapping of gold nanoparticles. For our equipment, the main trick to significantly expand the optical trapping range was to ensure that the laser beam was only expanded to slightly overfill the aperture of the objective; it was crucial that the tails of the Gaussian beam

* Corresponding author. E-mail: oddershede@nbi.dk. Telephone: 45 353 25287. Fax: 45 353 25425. Address: Niels Bohr Institute, Blegdamsvej 17, 2100 Copenhagen, Denmark.
[†] Niels Bohr Institute.
[‡] Nano-Science Center.

10.1021/nl051289r CCC: $30.25
Published on Web 08/31/2005

profile were not cut off by any optics. Also, a water immersion objective proved far more efficient than an oil immersion.

Also, we provide a quantitative analysis of the optical forces. The gold nanoparticles were trapped for a time long enough to allow for a three-dimensional description of how the strength of the trapping potential relates to the size of the gold nanoparticle. The lower size limit for trapping of gold nanoparticles was found to be 12 nm. Particles with this diameter could not be trapped for a time long enough to allow for a quantitative analysis. We did not, however, encounter an upper limit for the sizes of gold particles that could be optically trapped. The trapping potential was found to be harmonic in accordance with theoretical predictions. Escape force calibrations were performed to determine the largest optical forces that could be exerted on the gold nanoparticles. The magnitude of this force is of interest for the use of gold beads as nanoprobes.

Gold nanoparticles with mean diameters of 12, 18, 30, 40, and 72 nm were synthesized using the citrate reduction methods.[15,16] Details on these beads are given in Supporting Information. To prevent these small beads from aggregating, they were coated with bovine serum albumin (BSA). Because it is more difficult to produce larger particles with a narrow size distribution, we purchased the particles with $d = 101$ nm, $d = 154$ nm, $d = 196$ nm, and $d = 254$ nm (reported standard deviation on size is 10%) from British Biocell. These particles were not BSA stabilized because they were observed not to aggregate. The gold particles were suspended in water and sonicated for 15 min. A 30-μL perfusion chamber, consisting of two cover slips ($18 \times 18 \times 0.15$ mm^3 and $50 \times 25 \times 0.15$ mm^3) separated by vacuum grease, was used.

The optical trap was implemented in an inverted Leica microscope (Leica DMIRB HC) equipped with a quadrant photodiode (S5981, Hamamatsu) detection scheme[17,18] and a 25 Hz rate CCD camera (Sony XC-EI50). The trapping laser was a Nd:YVO_4 laser (10 W Spectra Physics Millennia, $\lambda = 1064$ nm, TEM_{oo}). The laser was focused to a diffraction-limited spot using a water immersion objective (HCX, PL, APO, 63×/NA = 1.2 Water Corr CS) or an oil immersion objective (HCX, PL, APO, 100×/NA = 1.4 oil CS). Data acquisition was performed by custom-made Labview programs. The condenser aperture was optimized to increase the sensitivity of the signal.[18,19]

For a quantitative analysis of the trapping strength, we simply recorded the time series of a gold nanoparticle performing Brownian motion in the optical trap. Escape force measurements were performed by oscillating a piezoelectric stage (PI 731.20, Physik Instrumente, Germany) with an amplitude of 10 μm and increasing the frequency until the particle escaped the trap. The temporal behavior of the variance of the voltage signal was found by calculating the variance in a running time window consisting of 4000 consecutive data points. The power spectrum analysis and fitting of histograms were performed using a Matlab software package specifically programmed for precise calibration of optical tweezers.[20]

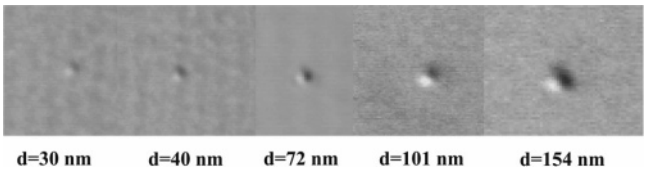

Figure 1. DIC images of gold beads stuck to a surface. The diameters of the beads are between 30 and 154 nm. Particles larger than this were directly observable in a bright field microscope.

The minimum laser power necessary to trap the gold beads depended on particle size and on which objective was used. The measurements reported here were performed at the lowest laser power providing stable optical trapping, this being in the range of 135−900 mW, measured at the output of the objective. The reported trap stiffnesses are all normalized with the corresponding laser powers used. The gold nanoparticles with $d \leq 72$ nm were not visible in bright-field microscopy with a 100× objective. However, by enhancing the contrast by using differential interference contrast microscopy (DIC), the particles could be seen on the CCD camera as shown in Figure 1. The particles were trapped simply by letting them diffuse into the optical trap, which was positioned 2−6 μm above the surface of the cover slip, thus avoiding proximity effects from the cover slip. If the suspension was not sufficiently dilute, more beads could diffuse into the trap during a measurement.

The forces acting on an optically trapped Rayleigh particle can be resolved into different contributions originating from scattering and absorption of a light incident on the sphere and gradient forces acting on the polarized sphere. Larger metallic particles are subject to radiometric forces caused by asymmetric heating of the particle,[21] but this contribution is small for Rayleigh particles.

Absorption and scattering forces destabilize axial trapping and make trapping of micrometer-sized metallic particles restricted to two dimensions.[11−13] However, for Rayleigh particles, the scattering and absorption cross sections are so small that the gradient force can exceed the scattering force in the axial direction, provided that there exists a large enough intensity gradient along the beam. The dielectric function of gold is a complex number $\epsilon_{gold} = \epsilon' + i\epsilon''$, the real and imaginary parts describing, respectively, the refraction and absorption of light in the metal. At 1047 nm, $\epsilon_{gold} = -54 + i5.9$[9] and the skin depth of gold is $\delta = 23$ nm; particles with radius $r \ll \delta$ are uniformly polarized by the light. As our wavelength is 1064 nm, we will use these values throughout. At wavelengths closer to the resonance of the surface plasmons, gold becomes much more absorptive and scattering more important. The gradient force $\boldsymbol{F}_{\mathbf{grad}}$ was therefore assumed to be the same as for a dielectric particle of equal size with polarizability, α, given by the Claussius−Mossotti relation

$$\alpha = \alpha' + i\alpha'' = V\frac{\epsilon_{gold} - \epsilon_w}{\epsilon_{gold} + 2\epsilon_w} \qquad (1)$$

Here, $\epsilon_w = 1.33^2$ is the dielectric constant of water at $\lambda =$

1064 nm, and V is the volume of the particle. To apply eq 1 to particles with $r \geq \delta$, one has to correct for the attenuation of the field inside the particle. The contributions to the optical forces are[9]

$$\boldsymbol{F}_{\mathrm{abs}} = \frac{n_{\mathrm{m}}\langle \boldsymbol{P} \rangle C_{\mathrm{abs}}}{c} \tag{2}$$

$$\boldsymbol{F}_{\mathrm{scat}} = \frac{n_{\mathrm{m}}\langle \boldsymbol{P} \rangle C_{\mathrm{scat}}}{c} \tag{3}$$

$$\boldsymbol{F}_{\mathrm{grad}} = \frac{|\alpha|}{2}\nabla\langle \boldsymbol{E}^2 \rangle \tag{4}$$

where $C_{\mathrm{abs}} = k\alpha''$ and $C_{\mathrm{scat}} = k^4|\alpha|^2/(4\pi)$ are the scattering and absorption cross sections of the gold particle, respectively. $k = 2\pi n_{\mathrm{m}}/\lambda$ is the wavenumber in the liquid, $\boldsymbol{P}$ is the Poynting vector of the electromagnetic wave, and n_{m} is the refractive index of the surrounding medium.

For a Gaussian intensity profile, the potential experienced by a particle near the focus is approximately harmonic in 3D. In one dimension (1D), the force is therefore given by Hook's law, $F = -\kappa(x - x_{\mathrm{o}})$, where x is the position of the particle, x_{o} is its equilibrium position, and κ is the stiffness of the trap. Also, the bead is subject to a frictional force from the surrounding liquid as well as stochastic forces, altogether resulting in Langevin's equation of motion. Fourier transformation of the Langevin equation gives a Lorentzian power spectrum from which, for example, κ can be determined.

We were able to trap gold colloids with diameters from 18 nm and up in diameter. Particles with $d = 12$ nm could not be trapped for a time long enough to permit a quantitative analysis even if the incident laser power was increased far above the level necessary to trap particles with a diameter 18 nm. Particles with $d = 18$ nm could be trapped only for less than one minute before escaping. The larger particles were easily trapped for considerably longer times.

To interpret the data from the quadrant photodiode, we assumed a linear relationship between the position of the bead and the detector signal in all three dimensions. This relation is given in refs 22 and 23 for dielectric particles. Our assumption regarding the smaller metallic beads is based on simulations of gold spheres,[19] $d < 300$ nm, showing that the positions and responses are linearly correlated.

A gold sphere fluctuating in a harmonic potential has a Gaussian distribution P of positions x,

$$P(x) = P_{\mathrm{o}}\, e^{[(-(x-x_{\mathrm{o}})^2/2\sigma^2)]} \tag{5}$$

where x_{o} is the position of the center of the trap, P_{o} is the expected number of times the particle will be observed at x_{o}, and the standard deviation, σ, is given by the equipartition theorem:

$$\sigma = \sqrt{\frac{k_{\mathrm{B}}T}{\kappa}} \tag{6}$$

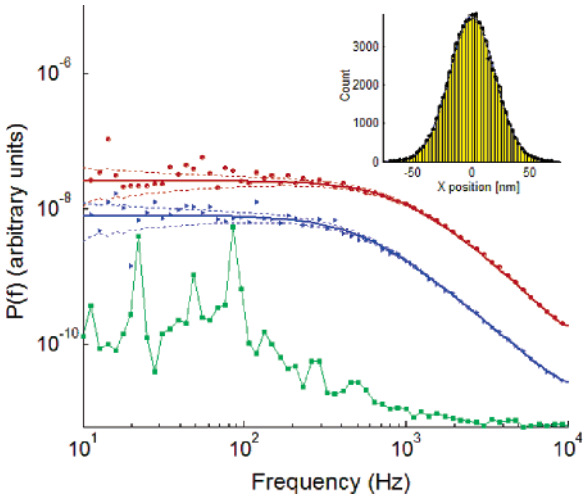

Figure 2. Position power spectra measured with water immersion objective. Red circles: gold particle, $d = 196$ nm, $\kappa = 0.011$ pN/nm ($P = 135$ mW). Blue triangles: gold particle, $d = 30$ nm, $\kappa = 0.00094$ pN/nm ($P = 450$ mW). Green squares: noise spectrum from an empty trap. Full lines are fits using the routines from ref 20. Dashed lines show the standard deviation of the blocked data points, which are Gaussian distributed around their expectation value (full line). The inset shows the distribution of positions for the 196 nm particle, full line shows fit of eq 5.

If the above-mentioned linear relationship between position and quadrant photodiode signal holds, the measured positions should have a Gaussian distribution. As shown in the inset of Figure 2, this is indeed the case; the full line in the inset is a fit of eq 5 to the position histogram for a $d = 196$ nm particle.

Because of filtering effects due to the photodiode, the Lorentzian form of the power spectrum is modified to account for this effect[24] as well as for aliasing and hydrodynamic corrections.[25] The power spectral data from two different sizes of gold beads as well as the fits are shown in Figure 2.

If the suspension was not sufficiently dilute, often more than one gold bead would diffuse into the trap. If one plots the variance of the position histogram as a function of time, there is a clear jump in the variance each time a new gold bead enters the trap. Such a "staircase" time series of the variance is shown in Figure 3, which is obtained during trapping of $d = 40$ nm gold particles. Probably, the variation in size of the gold beads is the reason for the levels of the variance not being perfectly equidistant.

To get a quantitative measure of the optical trapping strength, we determined the trap stiffnesses, κ_x, κ_y, and κ_z, in three dimensions and investigated how they depend on bead size. The trap is nearly symmetric in the directions perpendicular to the propagation of the laser light, hence $\kappa_x \approx \kappa_y$. However, in the direction parallel to the propagation of the laser light, the trap stiffness is substantially weaker. As $\boldsymbol{F}_{\mathrm{grad}}$ is proportional to laser power and because the laser power was varied from one particle size to another, κ was normalized with laser power measured at the sample. Figure 4 shows the normalized trapping strength (κ_x/power) in the direction perpendicular to the propagating laser beam as a function of bead radius.

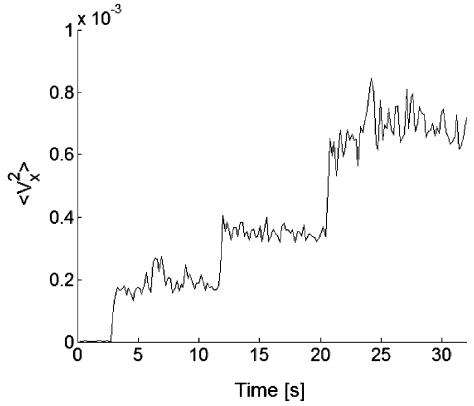

Figure 3. The variance of the signal from the photodiode recorded while successive gold particles, $d = 40 \pm 6$ nm, diffuse into the trap.

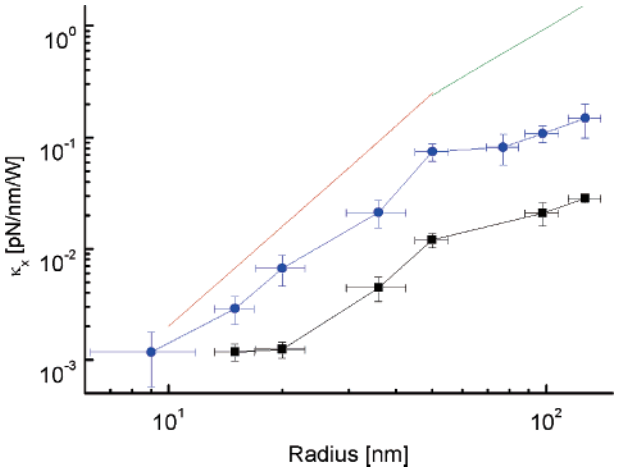

Figure 4. Double log plot of normalized trapping strength (κ_x/power) in the direction perpendicular to the trapping laser light as a function of radius of gold particles. Blue circles: trapping strength measured with a water immersion objective. Black squares: measured with an oil immersion objective. Each data point represents an average of 10−30 measurements. The red and green lines are drawn with slopes of, respectively, 3 and 2 for comparison.

It is clear from Figure 4 that the normalized perpendicular trapping strength increases with radius of the gold bead. Also, it appears as if the increase of the trapping strength is proportional to r^3 for particles with radius smaller than 50 nm. From eq 4, it is seen that $F_{grad} \propto \alpha$, and for small particles where the entire particle is fairly uniformly polarized, α is proportional to the volume V of the bead. However, for radii larger than the skin depth, the field intensity will decay exponentially inside the particle. Therefore, it is reasonable that the gradient force is observed to increase as r^3 for the smallest particles (see Figure 4). Also, it is understandable that there is a crossover to a different regime when the radius becomes significantly larger than the skin depth. One possibility is that as the particle becomes bigger, only an outer shell (with thickness $\sim \delta$) is polarized and, hence, that F_{grad} and the trapping strength would increase as r^2. However, when comparing data points larger than $r =$ 50 nm to the line with slope of 2 in Figure 4, it seems that the results do not comply with this model. The larger the beads, the larger the cross sectional area and, hence, the larger

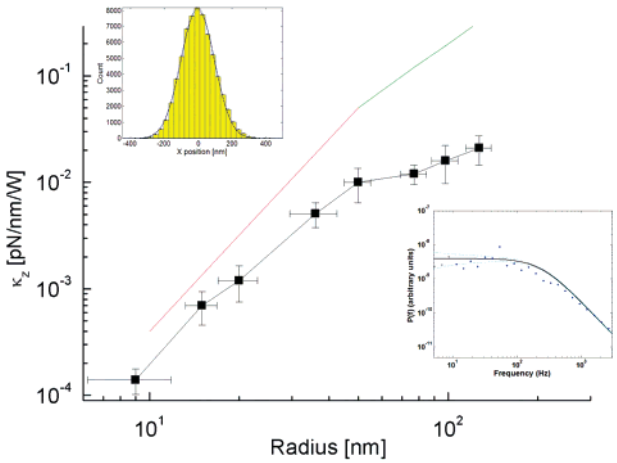

Figure 5. Normalized trapping strength in the direction parallel to the propagation of the laser light as a function of bead size. Upper inset shows the position histogram and the lower inset shows a typical power spectrum for a $d = 70$ nm gold bead. The red and blue lines with slopes of 3 and 2, respectively, are drawn for comparison.

the scattering force. This gives rise to an equilibrium position in the trap that is above the focus of the objective, and hence, the gradient force in the perpendicular direction cannot be expected to be as large as it would have been in the focus plane. This effect would give rise to a decrease of κ as a function of distance to the focus.

It is clear from Figure 4 that we were able to exert forces almost an order of magnitude larger by using the water immersion instead of the oil immersion objective. Qualitatively, the trapping strengths of the two different objectives had similar correlations to the radius of the trapped particles. One peculiarity is that we could not trap gold beads with $d = 154$ nm by using the oil objective. One clear disadvantage of the oil immersion objective is that it suffers from spherical aberrations.[10]

It appears (Figure 4) that, around $d = 100$ nm, there is a crossover between two regimes with qualitatively different behavior of the trapping strength as a function of bead size, and the scaling relation clearly changes. The size range above $d = 254$ nm was not explored, as gold particles of appropriate sizes were not available. Thus, we were not able to put an upper limit to the sizes of gold particles one can trap in 3D.

Figure 5 shows the results obtained from a similar analysis of the normalized trapping strength in the axial direction parallel to the propagating laser light. The upper left inset shows the position histogram and the lower right inset shows the power spectrum for a $d = 70$ nm bead in the trap. Thus, the thermal motion of the bead in the parallel direction is qualitatively identical to the perpendicular motion. Though the numbers are different, all the same conclusions can be drawn in the parallel direction as in the perpendicular direction. In particular, we note that, apparently, the normalized trapping strength increases with particle size. Data were obtained using a water immersion objective.

To exploit the depth and functional form of the trapping potential, we used the relations found in ref 26 for the electromagnetic field components derived from a fifth-order

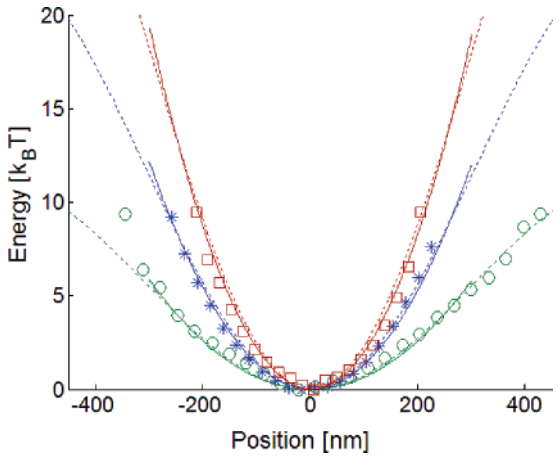

Figure 6. Potentials in the perpendicular direction. Circles: $d =$ 18 nm. Asterisk: $d = 30$ nm. Squares: $d = 40$ nm. Dotted lines are the theoretical predictions. Full lines are parabolic fits to the bottom of the theoretical potentials (dotted lines). Laser powers used: green, 855 mW; blue, 450 mW; red, 270 mW.

corrected Gaussian beam approximation. The energy was found by integrating $\boldsymbol{F}_{\mathbf{grad}}$ from eq 4 in the focus plane orthogonal to the propagating laser light. This simple procedure is only valid for approximately uniformly polarized particles such as Rayleigh particles. The potentials for the particles with $d = 18$, 30, and 40 nm are shown in Figure 6. The depth of the potential of a $d = 12$ nm particle at a laser power of 800 mW would be only $\sim 2k_BT$, thus explaining the difficulties with trapping this particle size. For a $d = 20$ nm particle under the same conditions, the depth of the potential is $\sim 12k_BT$. The symbols in Figure 6 show the measured potentials. Because the position distribution, $P(x)$, obeys Boltzmann statistics, the potential, U, can be found because $U \sim \ln[P(x)]$. The dotted lines are the theoretically predicted potentials and full lines are harmonic fits to the dotted lines, thus showing that the bottoms of the potentials are approximately harmonic. The data points lay fairly close to the theoretically predicted potentials. By knowing the potential depth U and the drag coefficient $\gamma = 6\pi\eta r$, the escape time, t, can be calculated from $\tau = \gamma/\kappa \exp(U/k_BT)$, which gives a typical escape time of $\tau = 30$ s for $d = 20$ nm particles at $P = 800$ mW. Because a trapped particle can only thermally probe the bottom of the potential well, we could not measure the complete potential. This type of analysis provides an alternative way of determining κ_x, and the results thus obtained are consistent with the previous analysis.

While trapping the smallest gold nanoparticles visible in bright-field microscopy ($d = 100$ nm), it was observed that two particles could be trapped next to each other in two separate potential minima. Also, two polystyrene particles with diameters ~300 nm could be trapped similarly next to each other. This phenomenon was more pronounced when using the oil rather than the water immersion objective and was observed using two totally independent optical trap setups. It appeared to be correlated to the polarization of the laser beam. This effect could be due to "optical binding", which is known to induce a periodic potential between two polarized particles in an optical trap.[27]

The maximum force that could be exerted on the particles in the lateral direction was found using a Stokes drag calibration. For particles ranging from $d = 101-254$ nm, the maximum force was found to be in the interval 0.56−2.2 pN (the larger the particle, the larger the maximum force) using a laser power of 135 mW. Thus, the largest force exertable in our setup using the full laser power of 10 W (~4.5 W exiting the objective) would be ~30 pN. This value is of interest for investigations of nanosystems where the force−range is important. One such example could be the probing of living cell cytoplasm using gold beads conjugated to organelles.

We have extended the previously known range of stable 3D optical trapping of metallic nanoparticles to particles ranging from 18 to 254 nm in diameter. Forces up to tens of pico-Newtons were exerted on the particles. Also, we have shown that the larger the particle, the larger the gradient force exerted on the particle, this conclusion being valid for both the lateral and axial directions. We did not determine the upper size limit where optical trapping becomes impossible because of the scattering force. However, the literature reports that micrometer-sized particles cannot be trapped in 3D. For small particles, the trapping strength increases as radius cubed. Thus, the trapping strength is proportional to the polarizability of the bead as expected. However, for particles larger than $d = 100$ nm in diameter, there is a crossover to a different regime with a qualitatively different scaling behavior.

Acknowledgment. This work was supported by the BIOP Graduate School, the Molecular Biophysics Graduate School, the Carlsberg Foundation, and the Lundbeck Foundation.

Supporting Information Available: Characterization of BSA-protected $d = 30$ nm gold nanoparticles. Average size, standard deviation, and SPR absorption max for the size series of BSA-covered gold nanoparticles. Pictures of gold nanoparticle solutions with diameters 12, 18, 30, 40, and 72 nm. This material is available free of charge via the Internet at http://pubs.acs.org.

References

(1) Xiao, Y.; Patolsky, F.; Katz, E.; Hainfeld, J. F.; Willner, I. *Science* **2003**, *299*, 1877−1881.
(2) Park, S.-J.; Taton, T. A.; Mirkin, C. A. *Science* **2002**, *295*, 1503−1506.
(3) Hamad-Schifferli, K.; Schwartz, J. J.; Santos, A. T.; Zhang, S.; Jacobson, J. M. *Nature* **2002**, *415*, 152−155.
(4) Hassenkam, T.; Moth-Poulsen, K.; Stuhr-Hansen, N.; Norgaard, K.; Kabir, M. S.; Bjornholm, T. *Nano Lett.* **2004**, *4*, 19−22.
(5) Sako, Y.; Kusumi, A. *J. Cell Biol.* **1995**, *129*, 1559−1574.
(6) Curtis, J. E.; Koss B. A.; Grier, D. G. *Opt. Commun.* **2002**, *207*, 169−175.
(7) Melville, H.; Milne, G. F.; Spalding, G. C.; Sibbett, W.; Dholakia, K.; McGloin, D. *Opt. Express* **2003**, *11*, 3562−3567.
(8) Vossen, D. L. J.; Fific, D.; Penninkhof, J.; van Dillen, T.; Polman, A.; van Blaaderen, A. *Nano Lett.* **2005**, *5*, 1175−1179.
(9) Svoboda, K.; Block, S. M. *Opt. Lett.* **1994**, *19*, 930−932.
(10) Rohrbach, A.; Stelzer, E. H. K. *Appl. Opt.* **2002**, *41*, 2494−2507.
(11) Furukawa, H.; Yamaguchi, I. *Opt. Lett.* **1998**, *23*, 216−218.
(12) Chun Ke, P.; Gu, M. *Appl. Opt.* **1999**, *38*, 160−167.
(13) Sato, S.; Harada, Y.; Waseda, Y. *Opt. Lett.* **1994**, *19*, 1807−1809.

(14) Sugiura, T.; Okada, T.; Inouye, Y.; Nakamura, O.; Kawata, S. *Opt. Lett.* **1997**, *22*, 1663−1665.
(15) Frens, G. *Nature Phys. Sci.* **1973**, *241*, 20−22.
(16) Turkevich, J.; Stevenson, P. C.; Hillier, J. *Discuss. Faraday Soc.* **1951**, *11*, 55−75.
(17) Oddershede, L.; Grego, S.; Nørrelykke, S. F.; Berg-Sørensen, K. *Probe Microsc.* **2001**, *2*, 129−137.
(18) Kisbye, J. D.; Berg-Sørensen, K.; Oddershede, L. *Appl. Opt.* **2004**, *43*, 1991−1996.
(19) Rohrbach, A.; Kress, H.; Stelzer, E. H. K. *Opt. Lett.* **2003**, *28*, 411−413.
(20) Hansen, P. M.; Tolicì-Nørrelykke, I. M.; Flyvbjerg, H.; Berg-Sørensen K. Tweezercalib 2.0: Faster Version of Matlab Package for Precise Calibration of Optical Tweezers. *Comput. Phys. Commun*. **2005**, submitted.
(21) Lewittes, M.; Arnold, S.; Oster, G. *Appl. Phys. Lett.* **1982**, *40*, 455−457.
(22) Gittes, F.; Schmidt, C. F. *Opt. Lett.* **1998**, *23*, 7−9.
(23) Pralle, A.; Prummer, M.; Florin, E. L.; Stelzer, E. H. K.; Horber, J. K. H. *Microsc. Res. Tech.* **1999**, *44*, 378−386.
(24) Berg-Sørensen, K.; Oddershede, L.; Florin, E.-L.; Flyvbjerg, H. J. *Appl. Phys.* **2003**, *93*, 3167−3177.
(25) Berg-Sørensen, K.; Flyvbjerg, H. *Rev. Sci. Inst*. **2004**, *43*, 1991−1996.
(26) Barton, J. P.; Alexander, R. D. *J. Appl. Phys.* **1989**, *66*, 2800−2802.
(27) Mohanty, S. K.; Andrews, J. T.; Gupta, P. K. *Opt. Express* **2004**, *12*, 2749−2756.

NL051289R